MAGNETIC PHAGOCYTE BIOSENSING FRAMEWORK FOR

POINT-OF-CARE SEPSIS DIAGNOSTICS AND MONITORING

By

COREY BENJAMIN NORTON

A thesis submitted to the

School of Graduate Studies

Rutgers, The State University of New Jersey

In partial fulfillment of the requirements

For the degree of

Master of Science

Graduate Program in Electrical and Computer Engineering

Written under the direction of

Umer Hassan

And approved by

_____

_____

_____

New Brunswick, New Jersey

May 2020

ABSTRACT OF THE THESIS

Magnetic Phagocyte Biosensing Framework for Point-of-Care Sepsis Diagnostics and Monitoring

by COREY BENJAMIN NORTON

Thesis Director:

Umer Hassan

Sepsis, a potentially deadly immunoresponse to infection, is a major concern in hospitals in the United States. Current laboratory processes used to diagnose and monitor sepsis are costly, time-consuming, or only provide a small piece of information about the complex condition. In order to develop specific individualized treatments for septic patients that do not heavily depend on the use of broad-spectrum antibiotics, a clinician must be provided with both pathogen information about the underlying infection and patient immunoresponse information. While there has been considerable progress towards biosensor designs that can provide pathogen information, there is still a significant demand for designs that can provide immunoresponse information.

The design of a novel biosensing framework has been proposed for gathering information about a patient's phagocytes, critical components of the innate immune system that protect the body from infection. The design is composed of electrical, microfluidic, and magnetic subsystems that work together to produce a distinct electrical signature signifying the presence of functional phagocytes in a human blood sample. The device has been simulated, fabricated, and experimentally tested using 17 blood samples collected from patients suspected of bacterial infections. Furthermore, two pattern recognition neural networks were developed to analyze and classify the experimental data. One network detects the presence of functional phagocytes in a

biological sample with 88.2% accuracy, and the other network diagnoses sepsis with 88.2% accuracy by analyzing these functional phagocytes. This novel framework presents the potential to reduce the mortality rate of sepsis by allowing for earlier diagnosis and treatment.

ACKNOWLEDGEMENTS

TABLE OF CONTENTS

LIST OF FIGURES

CHAPTER 1

INTRODUCTION

1.1 Sepsis

Sepsis is a common and potentially life-threatening condition in which the human immune system responds to an infection in a chemically unbalanced way, and it is the leading cause of death in hospitals in the United States. In the United States alone, more than one million people develop severe sepsis every year and between 200,000 and 500,000 people die as a result of this condition [1][2]. Although it can be caused by viral or fungal infections, sepsis is most often caused by bacterial infections present in the body and can result in the failure of multiple organs and organ systems. After onset, this condition can progress very quickly if left untreated, moving in increasingly fatal stages from mild sepsis to severe sepsis and finally septic shock [3][4].

Currently, clinical sepsis diagnosis often requires relatively expensive and sometimes time-consuming laboratory processing of blood samples. The most common sepsis biomarker used in clinical pathology labs is serum lactate, for which a concentration of greater than 2.0 mmol/L is indicative of septic shock [5][6]. Lactate is an organic molecule produced by the body's cells during anaerobic metabolism and has been shown to be present in higher concentrations for septic patients. While point-of-care devices do exist for blood lactate measurement, many hospitals often opt for central laboratory blood gas analyzers for improved accuracy [7]. These analyzers can cost on the order of thousands of dollars, and additional time is required to transport blood samples from the patient to the laboratory for processing in these machines.

Moreover, lactate concentration only provides information regarding a single aspect of a complex bodily dysfunction. While it is a useful metric for diagnosis, more information is

required to effectively treat the patient. Since sepsis is caused by the immune system's reaction to an infectious pathogen, information about both the pathogen and the patient's immunoresponse to it are helpful in devising treatment options. When a lack of this comprehensive information is present, typical clinical treatments for sepsis involve broad-spectrum antibiotics, which can lead to the development of antibiotic-resistance bacterial strains, ultimately making infections more difficult to combat in the future [8]. Careful detection and monitoring of both the specific pathogens present in a patient and the effectiveness of the patient's immunoresponse pathways in combatting that pathogen could allow for more tailored and individual treatment. Some strides have been made in rapid pathogen detection [9][10]. However, many aspects of a patient's immunoresponse information are still undetectable with currently available technologies.

1.2 Phagocytosis

Phagocytosis is a process by which phagocytic leukocytes, called phagocytes, attack invading pathogens in the body by engulfing and digesting them. It is the most critical function of the innate immune system and an important process to monitor in patients combatting infection [11][12]. As shown in Figure 1.1, this phagocytic process occurs in three main steps: recognition, internalization, and phagosome formation [13]. During the recognition phase, receptor molecules present on the membrane of phagocytic cells recognize and bind to ligands present on the surface of pathogenic cells. Once this recognition occurs, a biochemical signaling pathway is activated and the internalization phase begins. During this second phase, arm-like protrusions in the phagocyte's membrane called pseudopodia begin to surround the pathogen, binding more receptor molecules to the pathogen's ligands and gradually engulfing it. Once the pathogen has been entirely engulfed, the final phagosome formation phase begins. At this point, cytoskeletal reformation causes the plasma membrane around the pseudopodia to reconnect, completely internalizing the pathogen in a vesicle called a phagosome. After the completion of this

phagocytic process, the resulting phagosome matures into a phagolysosome, developing

biochemical properties that allow it to lyse the internalized pathogen [11][12][13].
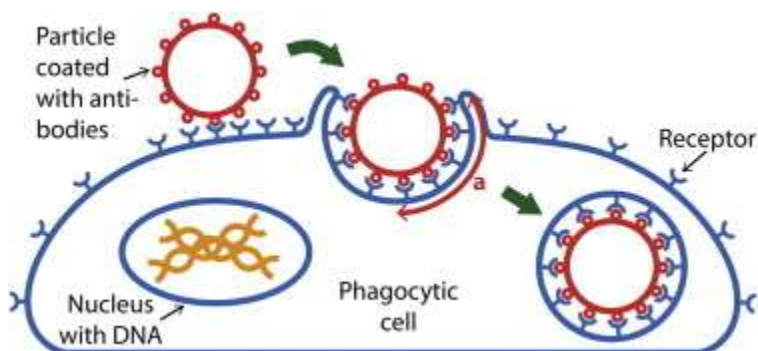
Figure 1.1: Diagram of phagocytic process including recognition, internalization and phagosome formation phases [13].

This innate immunoresponse is one of the human body's main defenses against

pathogenic infections. Therefore, detecting and quantifying a patient's capacity for performing

this process would provide clinicians with a critical piece of patient immunoresponse

information, potentially aiding in the development of patient-specific treatment. Several processes

have been proposed for making these measurements utilizing flow cytometry or classical

immunoassays [14][15]. However, these methods are too expensive and time-consuming to be

widely used in such common and time-sensitive cases as clinical sepsis monitoring. There is

currently no clinical test available to rapidly detect and quantify phagocytosis.

1.3 Point-of-Care Diagnostics

In recent years, an emphasis has been placed on the research and development of point-

of-care (POC) diagnostic devices for clinical settings [16][17][18]. These are medical devices that

can be used by clinicians to perform diagnostic biological measurements at the time and location

at which the patient is receiving care. This is in contrast with typical clinical diagnostic testing

that requires biological samples to be extracted from the patient and subsequently transported to a

medical laboratory to be processed. It can take hours or even days for a clinician to receive

laboratory results in this traditional manner, reducing the likelihood of survival for septic patients.

POC testing generally offers several crucial benefits when compared to traditional laboratory processes including a reduction in processing time, a reduction in sample volume, a reduction in overall cost, and an increase in portability [16][17][19].

1.3.1 Processing Time

POC devices present the potential to reduce the diagnostic sample-to-result time to a matter of minutes [19]. This can be a critical and life-saving improvement for time-sensitive diagnostic applications such as the testing and monitoring of sepsis because it allows for clinicians to begin treatment immediately, thereby increasing the likelihood of survival [3].

1.3.2 Sample Volume

In addition to reducing the time required to process a biological sample, POC devices can also reduce the volume of the sample to be processed. This is beneficial because standard phlebotomic practices of repeatedly drawing several milliliters of blood at a time have been shown to lead to iatrogenic anemia [20]. Furthermore, certain patients, such as neonates, inherently pose a higher risk of developing anemia and therefore pose a difficult challenge for clinicians to diagnose and monitor [21]. POC devices, however, only require sample volumes on the order of tens of microliters [19]. Performing diagnostic testing with these small sample volume devices can reduce the likelihood of developing iatrogenic anemia and increase the safety of diagnostic testing and monitoring.

1.3.3 Cost

Although patient safety and treatment are always the primary concern in the medical field, reducing the financial cost of diagnosis and treatment is a constant secondary concern. POC devices developed using microfluidic biosensors and lab-on-a-chip technologies can significantly reduce the instrumentation cost associated with diagnostic procedures [16][17][19]. In some cases, the reduction in cost can be so dramatic that devices can be developed for production costs

on the order of dollars or tens of dollars (USD) to replace traditional laboratory equipment with production costs on the order of thousands or tens of thousands of dollars (USD) [16] [22].

<u>1.3.4 Portability</u>

The inherent portability of POC diagnostic devices means that their utilization is not limited only to hospitals and medical laboratories as is the case with many traditional diagnostic tools [16][19]. POC devices can also be utilized in pre-hospital settings such as ambulances, nursing homes, rehabilitation centers and other outpatient facilities. Beginning diagnostic testing in these pre-hospital settings can encourage more immediate treatment when the patient arrives at a hospital, which again improves the likelihood of survival [3][23]. This is especially true for patients with quickly progressing conditions such as sepsis.

1.4 Statement of Problem

The current clinical processes for sepsis diagnosis and monitoring do not provide clinicians with enough information to develop individualized treatments for infected patients. In order to move away from broad-spectrum antibiotics and towards individualized treatments, both specific pathogen information and patient immunoresponse information must be made available. However, systems for rapidly acquiring important immunoresponse metrics from septic patients is currently lacking, the most important being phagocytic detection and quantification. The development of a POC device to perform such diagnostic measurements could potentially reduce the mortality rate of septic patients by facilitating early detection and treatment.

1.5 Organization of the Thesis

After highlighting the motivation behind the design of a POC diagnostic device for phagocyte detection in Chapter 1, the design of a microelectromechanical biosensing framework to achieve this goal and preliminary simulations of that framework are outlined in Chapter 2. In this chapter, each of the design's three constituent subsystems is explained individually. In

Chapter 3, the procedures used to fabricate the device are outlined, as well as the procedures used to prepare biological samples for device testing. In this chapter, a biological control assay is also proposed to validate the performance of the device. In Chapter 4, the instrumentation and signal processing techniques used to collect data from the device are outlined and the data is analyzed. Data analysis in this chapter is comprised of qualitative signal analysis, quantitative statistical analysis, and the development of a neural network for deep learning-based analysis. Finally, Chapter 5 summarizes the results of the study and outlines the future scope of the project.

CHAPTER 2

SENSOR DESIGN AND SIMULATIONS

2.1 Novel Biosensing Framework

A novel biosensing framework has been designed to detect the phagocytic capability of an infected patient's immune system. In addition to monitoring a patient's immunoresponse to a bacterial infection, this device can also be used as an alternative tool for sepsis diagnosis because the enhanced presence of phagocytic cells (particularly neutrophils) in the bloodstream has been shown to indicate the onset of sepsis [12]. The proposed in vitro design uses opsonized ferromagnetic microparticles to simulate the presence of bacterial cells in a human blood sample. These particles are roughly the size of an average bacterial cell (0.5 μm diameter) and are artificially coated in the same ligand that would be present on a bacterial cell. Because of this, the receptor molecules on the phagocytic cells in the sample bind to the particles, beginning the phagocytic process. However, since the particles are made of a non-organic ferrous material, they cannot be digested by the phagocyte and will instead remain indefinitely trapped within a vesicle.

The presence of ferromagnetic particles within functional phagocytes allows the cells to be manipulated by a magnetic field. Therefore, a magnetic field can be utilized to selectively alter the flow rate of functional phagocytes in a microfluidic system. This magnetic field can also be coupled with an impedimetric cell sensor in order to record this change as shown in Figure 2.1. A microelectromechanical POC framework has been developed to utilize this concept and can be explained by its three constituent subsystems: electrical, and microfluidic, and magnetic.
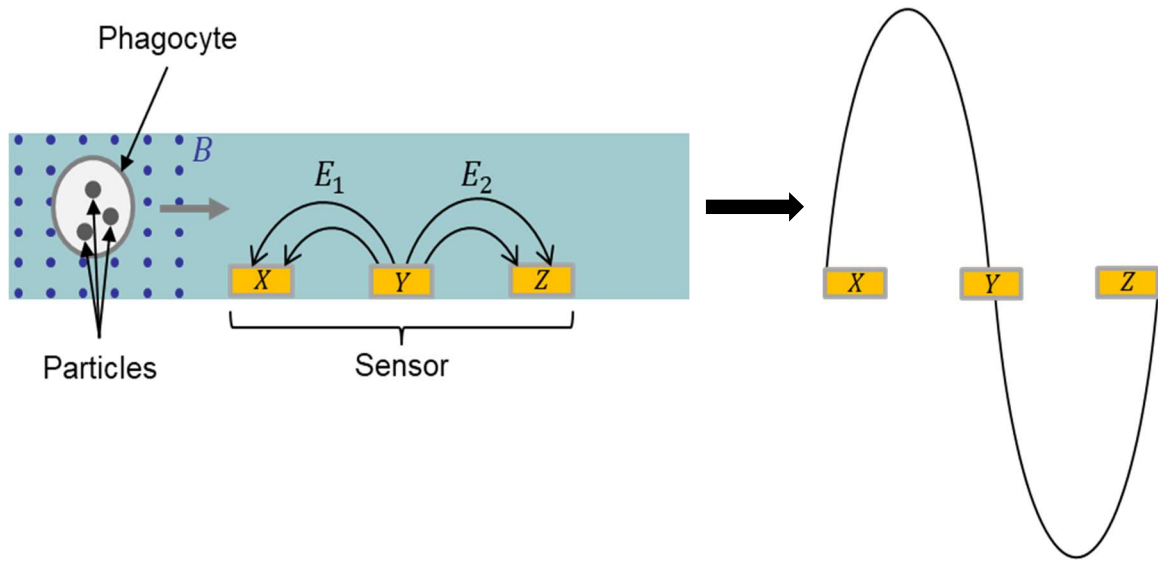
Figure 2.1: Biosensor Side View and Bipolar Pulse Generated by Passing Cell

2.1.1 Electrical Subsystem

The electrical subsystem of this design is comprised of three coplanar 100 μm by 100 μm gold electrodes with inter-electrode spacing of 150 μm on a glass substrate that function together as an impedimetric sensor. This sensor operates on the principle that a biological cell has a higher impedance than its surrounding fluid, which is relatively conductive. As shown in Figure 2.1, applying an AC voltage course to the electrode Y in the center generates electric fields between electrode Y and electrodes X and Z on either side. A current signal is measured from both electrodes X and Z. The difference between the two current signals is take in order to stabilize the baseline of the signal ($I_{diff} = I_{YX} - I_{YZ}$). When a cell disrupts one these electric fields, it introduces an increased impedance to the system which manifests itself as a change in the corresponding current signal. Assuming the sample flows through a linear microfluidic channel with no other paths, every cell would disrupt both electric fields in sequence, generating a bipolar pulse in the differential current signal as shown in Figure 2.1. The amplitude and width of this pulse contains information about the cell being analyzed, namely its volume and its flow speed.

2.1.2 Microfluidic Subsystem

The microfluidic subsystem is comprised of a single linear channel 100 μm in width and 50 μm in height with two focusing regions and inlet/outlet holes that constrict the width to 30 μm. The purpose of the microfluidic channel is to flow the biological sample of interest through the sensing region formed by the electrical subsystem in a controlled manner. By the intrinsic nature of the microscopic scale at which this channel is designed, the biological sample will experience laminar flow throughout the entirety of the channel, ensuring that the cells pass through the sensing region in a streamlined fashion. The two focusing regions of the channel are intended to lie between each pair of electrodes in the electrical subsystem as shown in Figure 2.2. Assuming the channel walls are fabricated with a non-conductive material, these regions will focus the electric field into a smaller volume of the conductive fluid, thereby increasing the current density in that constricted region. The increase in current density in the sensing region allows for an improved signal-to-noise ratio (SNR) in the measured differential current signal.
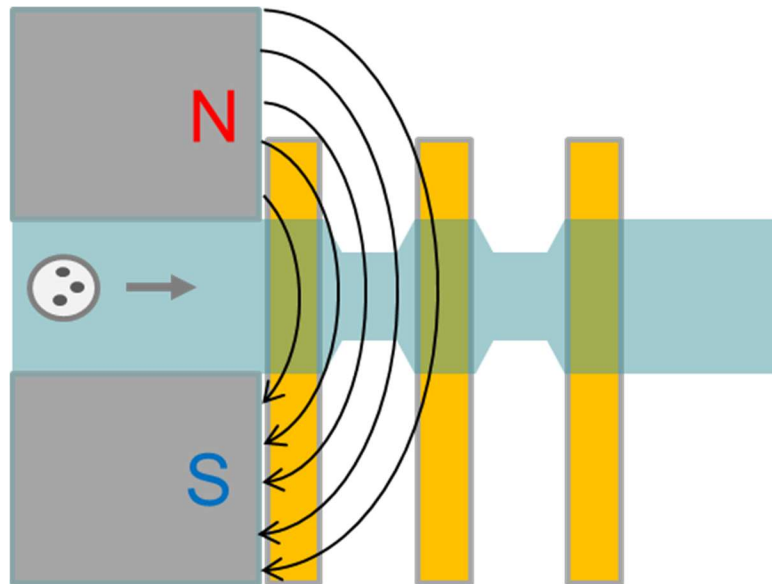
Figure 2.2: Biosensor Top View

2.1.3 Magnetic Subsystem

The magnetic subsystem is comprised of two permanent neodymium magnets with opposite polarities just upstream of the sensing region that provide a constant magnetic field in a portion of the microfluidic channel as shown in Figure 2.2. The purpose of this magnetic field is to alter the flow rate of phagocytes passing through the sensing region that have internalized ferromagnetic microparticles. As the microparticles come in close proximity to the magnetic field from upstream, they become polarized and magnetically attracted towards it. This increases the overall speed of the cell containing the particles and subsequently reduces the corresponding pulse width measured from the differential current. As the microparticles move downstream, away from the magnetic field, the polarized particles are still magnetically attracted towards the field. Now, this attractive force decreases the overall speed of the cell containing the particles, and subsequently increases the corresponding pulse width measured form the differential current. In this way, the magnetic subsystem causes a disruption of the sample flow due to the presence of functional phagocytes which can be measured by the electrical subsystem.
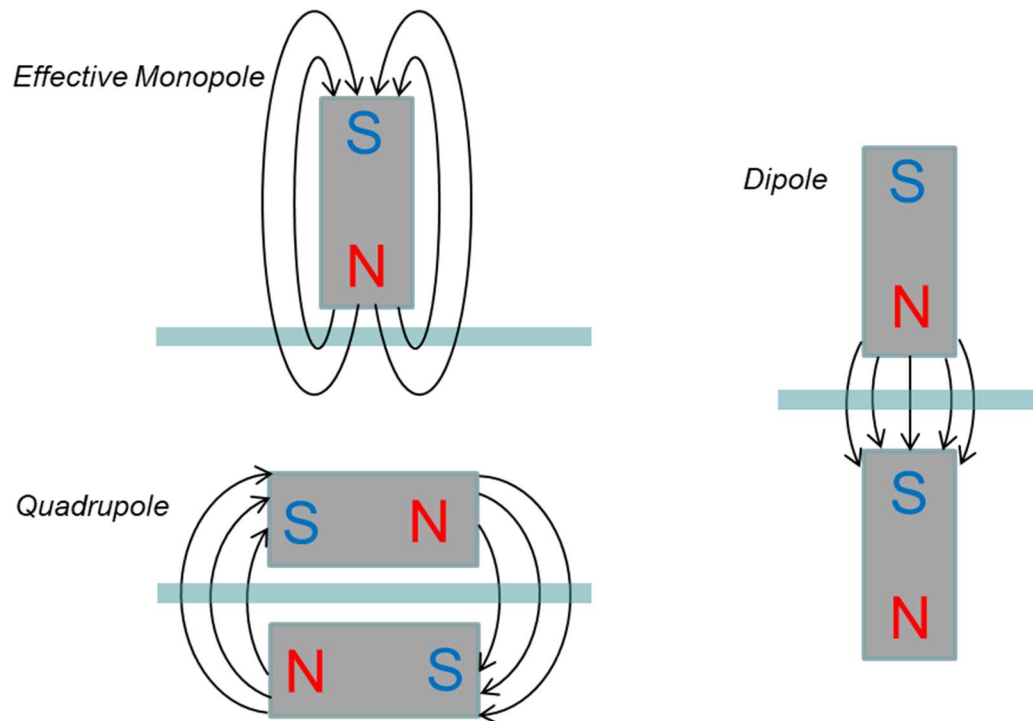
Figure 2.3: Effective Monopole, Dipole, and Quadrupole Magnetic Field Configurations

Several different configurations of permanent magnets were considered in order to determine which would be the most effective for this application: an effective monopolar configuration, a dipolar configuration, and a quadrupolar configuration as shown in Figure 2.3. Although a monopolar magnetic field cannot technically exist, the first configuration is considered to be "effectively monopolar" because the microfluidic channel is disproportionately close to one pole as compared to the other. This type of configuration provides the least uniform magnetic field throughout the channel and is therefore, non-ideal.

The dipole and quadrupole configurations, also shown in Figure 2.3, provide a much more uniform magnetic field throughout the channel. In these configurations, the north and south poles of two distinct permanent magnets are utilized in conjunction with one another to form a more complex magnetic field profile. The biggest difference between these two configurations is the volume of the channel affected by the magnetic fields. The quadrupole configuration provides a magnetic field which is strong at either end of the permanent magnets, and very weak anywhere else in the channel. This type of field profile is beneficial because it can be used to impose a force on the microparticles only in the sensing region, preventing the change in velocity caused by the magnetic force from overcoming the constant velocity derived from pressure-driven flow of the microfluidic system. This prevents the inadvertent capture of cells in the system and subsequent clogging of the microfluidic channel. For this reason, the quadrupole configuration was chosen for this design.

2.2 Design Simulations

Several theoretical simulations were performed to test the functionality of this design. First, electrical simulations were performed to ensure that the impedimetric counter functioned as intended and recorded a bipolar pulse in the differential current signal in response to a passing cell. Then, magnetic field simulations were performed to ensure that the field profile created by the permanent magnets provided high and low field strengths in the appropriate locations. Finally,

magnetic force simulations were performed to determine if the magnetic field generated by the permanent magnets would be capable of enacting a force on a cell with internalized ferromagnetic microparticles in the sensing region. All simulations were performed using COMSOL Multiphysics.

2.2.1 Electrical Simulations

A model of a microfluidic channel was created with a width of 15 μm and a height of 15 μm as shown in Figure 2.4. Three 15 μm by 15 μm coplanar electrodes are located at the bottom of this microfluidic channel with inter-electrode spacing of 15 μm. This model is intended to simulate the microfluidic and electrical subsystems, and more specifically the impedimetric sensor. In this model, the channel is filled with a conductive fluid with relative permittivity of 80 that is intended to mimic the phosphate-buffered saline solution in which the phagocytes will be suspended in the biosensor [24]. Additionally, a sphere with a diameter of 12 μm and a relative permittivity of 150.9 is located in the channel to mimic a neutrophil [25]. It should be noted that the structure and dimensions of both the microfluidic and electrical subsystems were changed for the final design. However, this simulation still serves as a proof-of-concept for the impedimetric sensor.
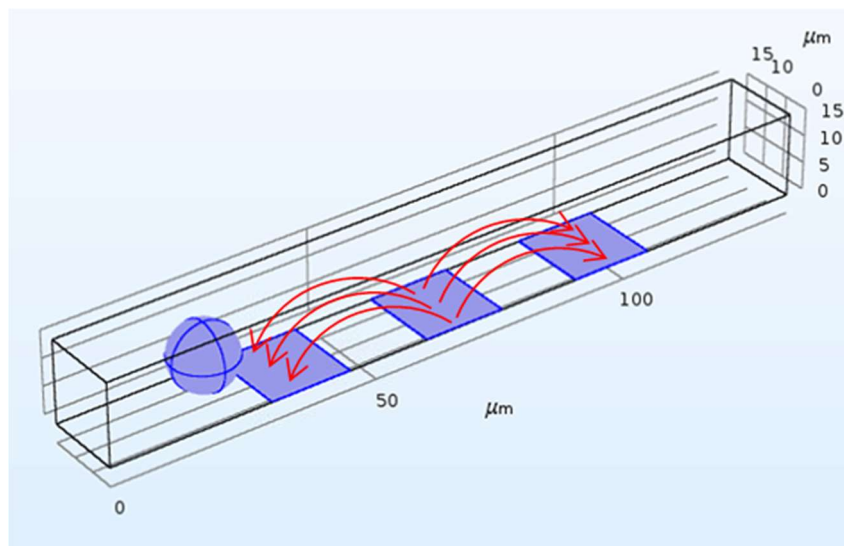
Figure 2.4: Coplanar Electrode Model

Using this model, a simulation was performed to mimic the flowing of a neutrophil through the sensing region. To do this, the location of the sphere representing the neutrophil was parameterized and swept through the sensing region in 5 μm increments. During this time, a 5V 300 kHz AC voltage signal was applied to the middle electrode and the voltage was measured at each of the outer two electrodes. The two voltages were subtracted, and the differential voltage was plotted across all swept phagocyte locations to receive the bipolar pulse described earlier in this chapter. The results of this simulation are shown in Figure 2.5
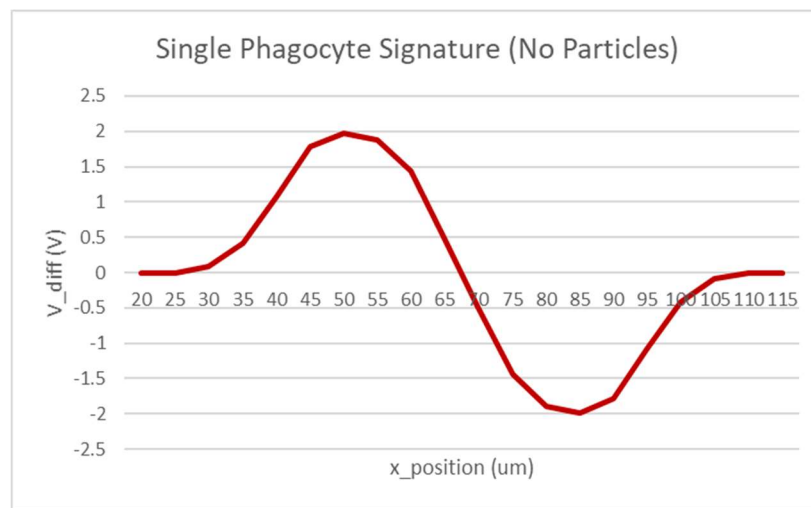
Figure 2.5: Simulated Electrical Signature of a Phagocyte

2.2.2 Magnetic Field Simulations

In order to simulate the magnetic field generated by the magnetic subsystem, a model was created with two permanent magnets of opposite polarities on either side of a linear microfluidic channel as shown in Figure 2.6. For this simulation, the same microfluidic channel and conductive fluid used during the electrical simulations were used again. The magnets on either side of the channel have a width of 300 μm, a height of 150 μm, and a depth of 150 μm and are meant to represent a section of a larger magnet. For this simulation, the profile of the magnetic field was more critical than its value, so the magnetization of each permanent magnet

was arbitrarily chosen to be 31.5 MA/m in order to roughly match the magnetization of the commercially available permanent magnets that would ultimately be used in the final design. The magnetic field profile matched the expected profile of a quadrupole configuration as described earlier in this chapter as shown in Figure 2.7.
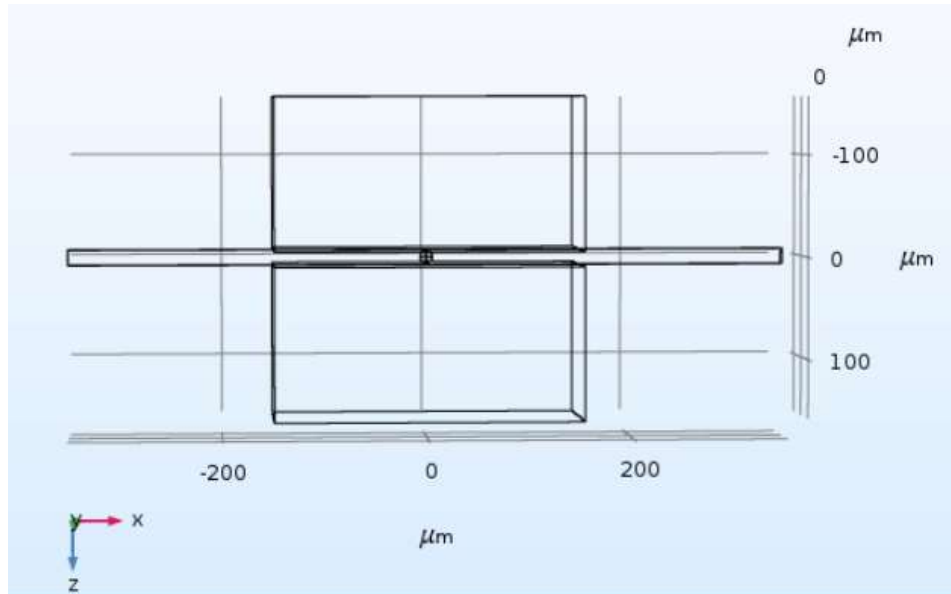
Figure 2.6: Magnetic Field Model
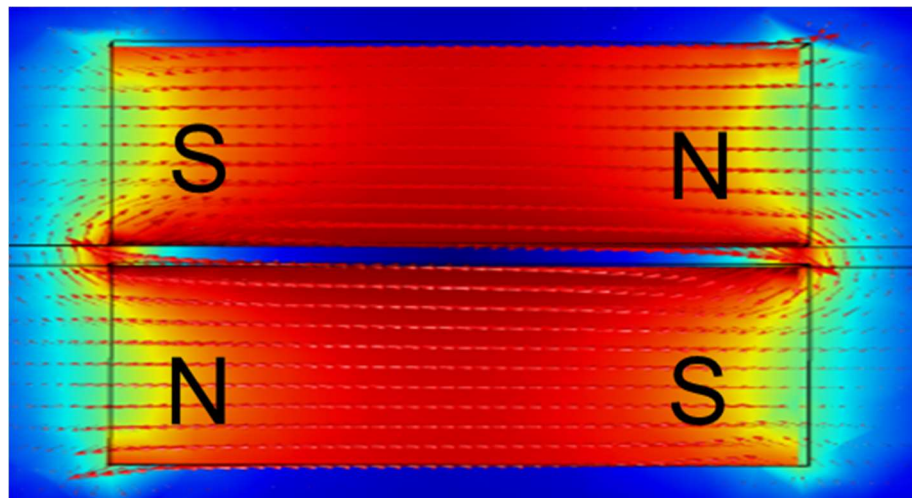
Figure 2.7: Simulated Quadrupole Magnetic Field

<u>2.2.3 Magnetic Force Simulations</u>

A sphere with a diameter of 12 μm was introduced to the magnetic field simulations from the previous section in order to simulate a neutrophil. Additionally, a smaller sphere with a diameter of 1 μm was added inside the neutrophil to simulate a phagocytosed ferromagnetic microparticle. The location of the neutrophil and its internalized microparticle was parameterized and swept across the length of the channel in 1 μm increments. At each increment, the magnetic force acting on the microparticle by the permanent magnetic field was recorded and plotted as shown in Figure 2.8. As expected, the quadrupole magnetic field configuration enacted a strong magnetic force on the microparticle, and by extension on the neutrophil, only at the edges of the permanent magnets and very little magnetic force elsewhere in the channel. The seemingly unpredictable nature of the directional component of the magnetic force in these results can be attributed to the lack of conservation of particle polarization between parametric steps and is a limitation of the COMSOL modules available for this study.
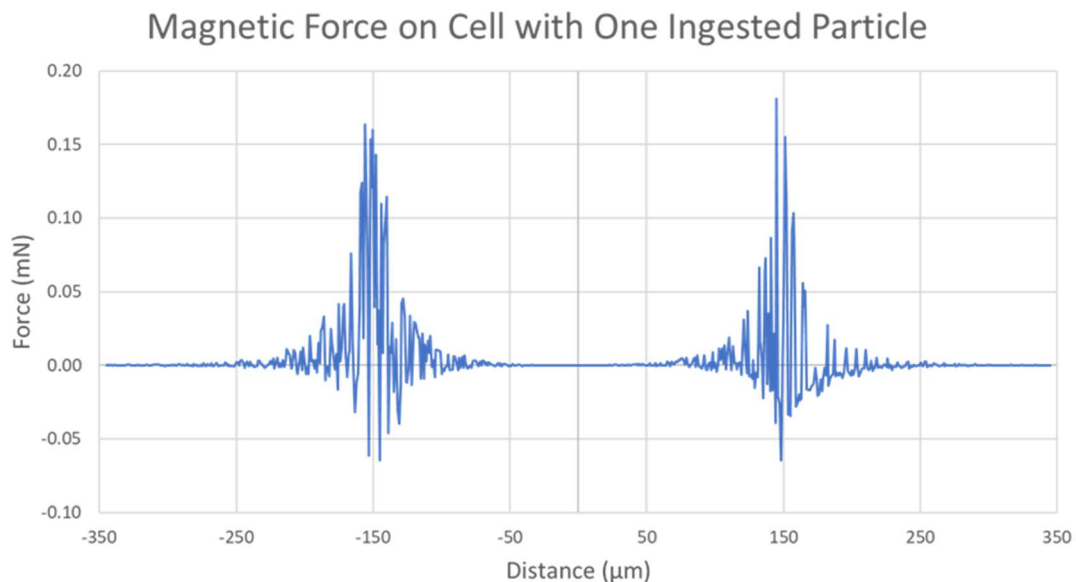
Figure 2.8: Simulated Magnetic Force on Phagocyte with a Single Internalized Microparticle

To take this simulation a step further, the process was repeated for different quantities of internalized microparticles from 1 to 10 and the peak magnetic force was recorded each time. The results of this study are shown in Figure 2.9. As expected, the peak magnetic force acting on the phagocyte generally increases with the number of internalized particles. The fact that the force did not increase at every increment can be explained by the fact that each particle exists at a different location in the phagocyte and is therefore acted upon by the magnetic field at slightly different increments along the channel. For instance, a particle at the front of the cell will pass the edge of the magnets before a particle at the back of the cell. This can result in two different particles pulling the same cell in opposite directions. Therefore, depending on the orientation of the particles within the cell, the peak magnetic force may not always increase with an increasing number of internalized particles even though this is true as a general trend
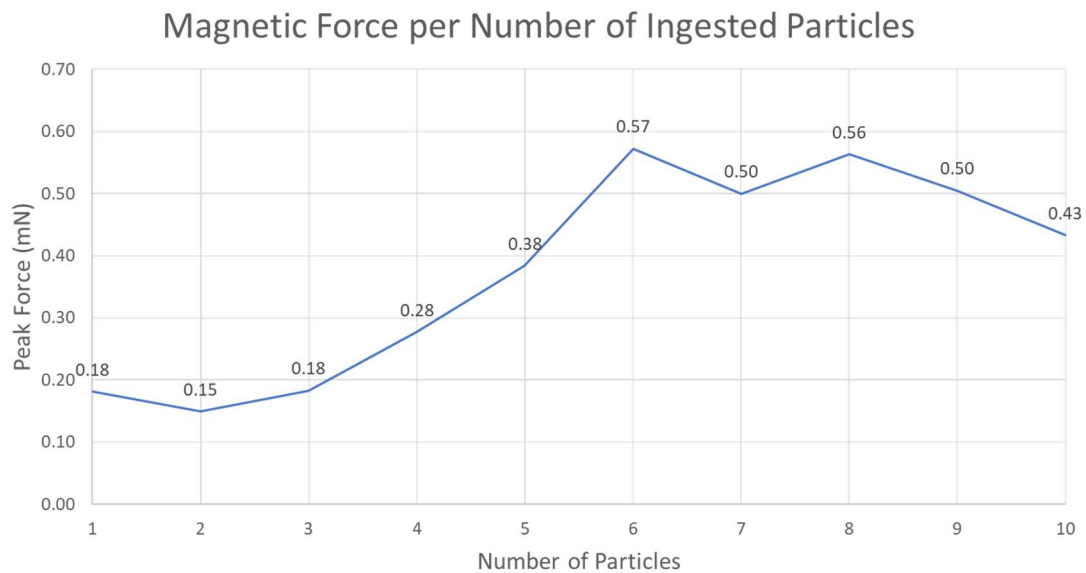
Figure 2.9: Peak Magnetic Force as a Function of the Number of Internalized Microparticles

In addition to the number of internalized microparticles, the magnetization of the permanent magnets was parameterized. This property was swept from 0 to 50 MA/m in 5 MA/m increments while keeping the number of internalized microparticles at a constant 1 and the peak magnetic force was recorded for each step. The results of this study are shown in Figure 2.10. As

expected, the peak magnetic force acting on a phagocyte with a single internalized ferromagnetic microparticle increased with increasing magnetization of the permanent magnets used to form the quadrupole magnetic field. The results show a very clear exponential relationship between the magnetization of the permanent magnets and the peak magnetic force acting on the phagocyte. This is useful, because it allows for well-defined control over the magnetic force in the final design by changing the strength of the magnets used.
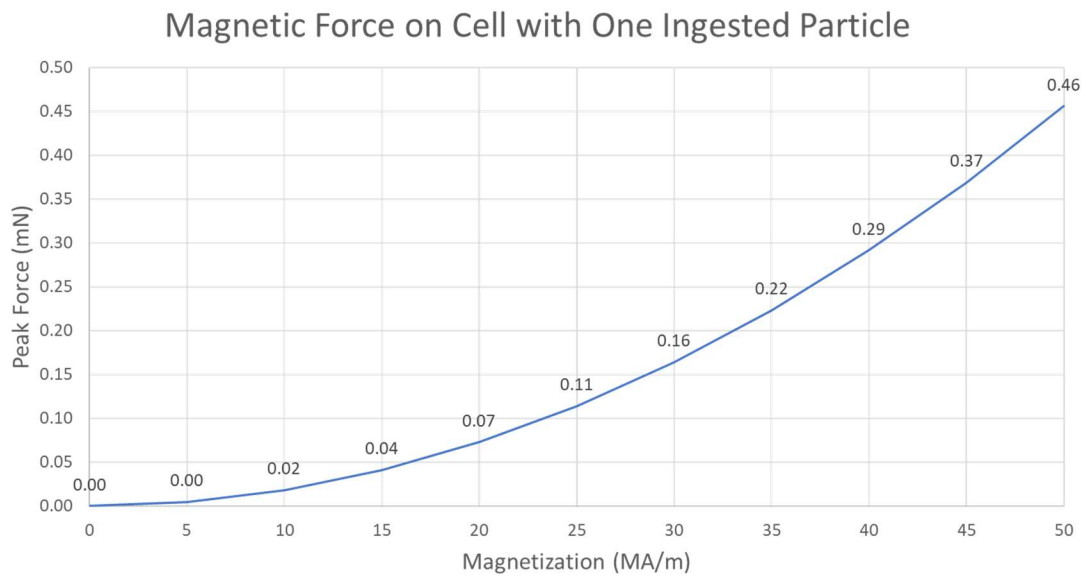
Figure 2.10: Peak Magnetic Force as a Function of Magnetization

CHAPTER 3

DEVICE FABRICATION AND SAMPLE PREPARATION

3.1 Microfluidic Channel Fabrication

The microfluidic subsystem of this device was fabricated using a combination of traditional photolithographic and soft lithographic microfabrication techniques. To begin, a master mold is fabricated on a silicon substrate. This mold is then used to repeatedly fabricate microfluidic devices made of a silicone elastomer called polydimethylsiloxane (PDMS). These fabrication processes are explained in detail below but can also be seen in a simplified manner in Figure 3.1.

Negative photoresist is spun onto the substrate → Substrate is selectively exposed to UV light → Substrate is patterned by UV exposure → PDMS is poured onto the substrate → PDMS is hardened and lifted from the substrate
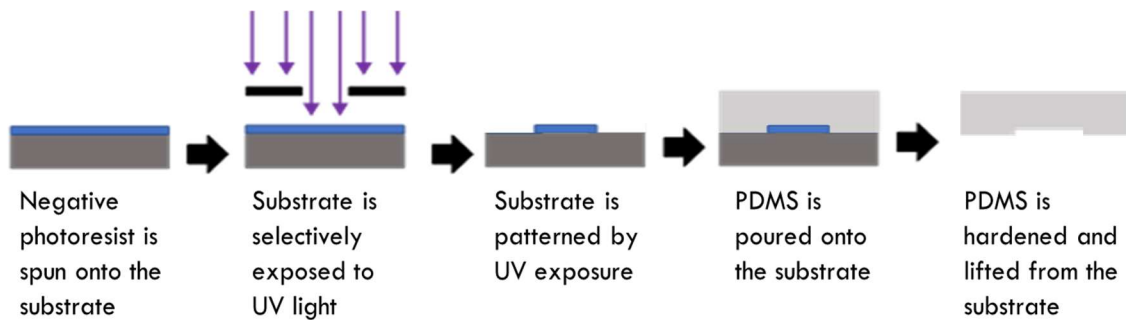
Figure 3.1: Microfluidic Subsystem Fabrication Process

3.1.1 Master Mold Lithography

Before the master mold fabrication begins, the silicon wafer that will serve as a substrate is thoroughly cleaned and prepared for lithography by consecutively soaking it in baths of acetone, isopropyl alcohol, and de-ionized water for 10 minutes each, drying it with compressed nitrogen gas, and baking the wafer for 30 minutes at 150°C. After the wafer is cleaned, baked, and allowed to cool for an additional five minutes, SU-8 2025 negative photoresist is spin-coated onto the wafer to provide an even layer across the surface. Then, the wafer is baked for 5 minutes at 65°C and 60 minutes at 95°C consecutively.

At this point, the wafer is ready to be patterned by selective exposure to ultraviolet light. This is achieved by using a commercially fabricated photomask that has been designed to allow light to pass only in the regions where the channels are desired. The masked used for this process has been designed to pattern 8 microfluidic channels on a single silicon wafer. Before exposure, this photomask is also cleaned using acetone, isopropyl alcohol, de-ionized water, and compressed nitrogen gas. The SU-8 photoresist is then exposed through the photomask to ultraviolet light with a dose of 450 mJ/cm^2. The exposed wafer then undergoes another two-step bake process in which it is baked for 2 minutes at 65°C and 6 minutes at 95°C consecutively.

At this point, the portions of SU-8 that have been exposed to ultraviolet radiation become insoluble and the unexposed regions become more soluble. The wafer is submerged in an SU-8 developer solution and allowed to develop on a shaker plate for approximately 20 minutes, which dissolves the soluble un-exposed regions of the photoresist and leaves only photoresist in the regions where the microfluidic channels are desired. The wafer is then rinsed with de-ionized water and dried with compressed nitrogen gas. Finally, it is placed in a desiccator under vacuum along with 20 μL of trichlorosilane to form a silane layer overtop it that acts as a coupling layer between the silicon substrate and the PDMS used in the next fabrication process.

3.1.2 PDMS Soft Lithography

Once the master mold has been fully fabricated, soft lithography techniques can be used to fabricate the microfluidic devices. First, the PDMS elastomer base and its activator are combined in a 10:1 ratio and manually mixed until a viscous homogeneous solution is formed. Then, homogeneous elastomer solution is poured over the master mold in a petri dish until it covers the wafer with the desired thickness. In order to remove any bubbles than may have formed during the mixing and pouring process, the entire petri dish is desiccated under vacuum for 1 hour. Once all bubbles have been removed from the PDMS solution, the wafer is baked overnight at 65°C to polymerize and solidify.

Once the PDMS has been molded into the silicon master mold, the 8 individual

microfluidic devices are individually cut out from the master mold using a scalpel. Inlet and

outlet holes are carefully formed at either end of the linear channel using a biopsy needle. At this

point, the microfluidic subsystem fabrication is complete.

3.2 Electrode Fabrication

The electrical subsystem of this device was also fabricated using traditional

photolithographic microfabrication techniques, this time for patterning gold on a glass substrate.

These fabrication processes are explained in detail below but can also be seen in a simplified

manner in Figure 3.2. For this process, the glass wafer was cleaned and baked according to the

same process as was used for the silicon wafer during the microfluidic master mold fabrication.

After cleaning, baking, and cooling, the glass wafer is spin-coated once with

hexamethyldisilazane (HMDS) and then again with Shipley S1818 positive photoresist. The

HMDS here acts as an adhesion promoter between the glass substrate and the Shipley photoresist.

The wafer is then baked for 4 minutes at 120°C.

Substrate is patterned using positive photoresist

Gold film is deposited on the wafer

Photoresist is removed, along with the unwanted portions of the gold film
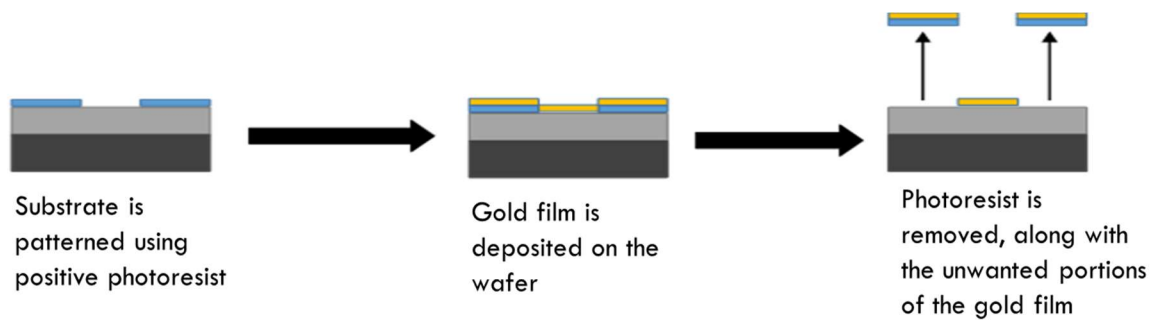
Figure 3.2: Electrical Subsystem Fabrication Process

At this point, another photomask is used to pattern the electrodes into the photoresist

using ultraviolet light. Similarly to the mask used for the microfluidic master mold, this

photomask is designed to pattern 8 sets of electrodes on a single glass wafer. The photomask is

cleaned according to the same protocol used during the microfluidic master mold fabrication and

the glass wafer is selectively exposed to ultraviolet radiation with a dose of 350 mJ/cm^2. This

time, only the regions exposed to the ultraviolet radiation become soluble, and all other regions remain insoluble. No post-exposure bake is required for this photoresist. The wafer is submerged in MF-319 developer solution and allowed to develop on a shaker plate for 20 minutes, which now dissolves the photoresist only in the regions where the electrodes are desired. Again, the wafer is rinsed with de-ionized water and dried with compressed nitrogen gas after development. Oxygen plasma is also used to descum the wafer after development as an additional cleaning step to remove photoresist residue.

Before depositing the gold onto the wafer, the exposed regions of the glass wafer are etched to ensure a flush edge between the glass substrate and the gold electrodes. To perform this etching, the wafer is soaked in hydrofluoric acid for 5 minutes and then thoroughly rinsed with de-ionized water. During this process, the remaining photoresist protects the glass underneath it from being etched, so only the glass in the locations of the desired electrodes is etched. After etching, a 10 nm layer of chromium is sputtered onto the glass substrate, followed by a 100 nm layer of gold. Gold is used to fabricate the electrodes because it is inert and resistant to corrosion, and chromium is used to improve the adhesion between the gold and the glass substrate. At this point the remaining photoresist, along with the gold layer above it, is lifted-off from the glass wafer using acetone and the wafer is cleaned using isopropyl alcohol, de-ionized water, and compressed nitrogen gas. All that remains on the glass wafer is gold in the regions where the electrodes are desired as shown in Figure 3.3, and the 8 individual sets of electrodes are separated using a dicing saw.
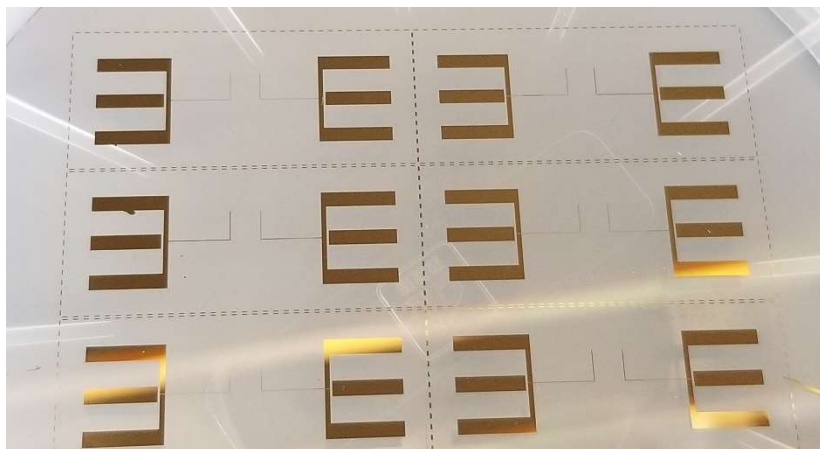
Figure 3.3: Image of Fabricated Gold Electrodes

3.3 Subsystem Integration

Once both the electrical and microfluidic subsystems have been individually fabricated, they are ready to be combined along with the magnetic subsystem to form the complete biosensor framework. To do this, the PDMS microfluidic devices must be chemically bonded to the glass substrate of the electrodes. However, both subsystems must be thoroughly cleaned prior to bonding to ensure the channel maintains an airtight seal. Both subsystems are submerged in ethanol and sonicated for 20 minutes to remove any debris. They are then rinsed in de-ionized water and dried with compressed nitrogen gas. Once sufficiently cleaned, both subsystems are exposed to oxygen plasma, carefully aligned to each other so that the focusing regions lie between the electrodes as shown in Figure 3.4 and left to cure overnight. The oxygen plasma here facilitates covalent bonding between the PDMS of the microfluidic subsystem and the glass substrate of the electrical subsystem. It is important to recognize that a misalignment of the microfluidic channel during this step will result in a reduction of the SNR experienced by the system. At this point, the microfluidic and electrical subsystems are fully integrated as shown in Figure 3.5.
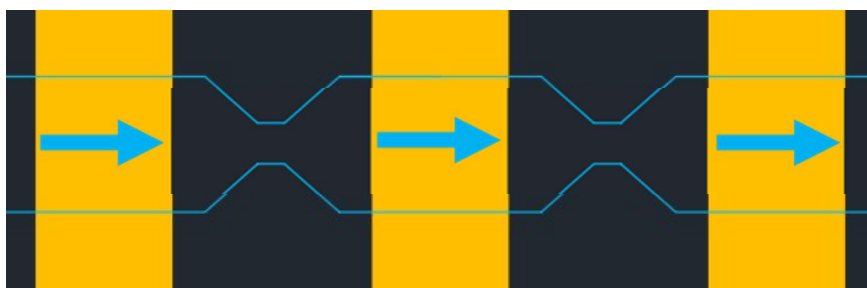
Figure 3.4 Alignment of Microfluidic and Electrical Subsystems
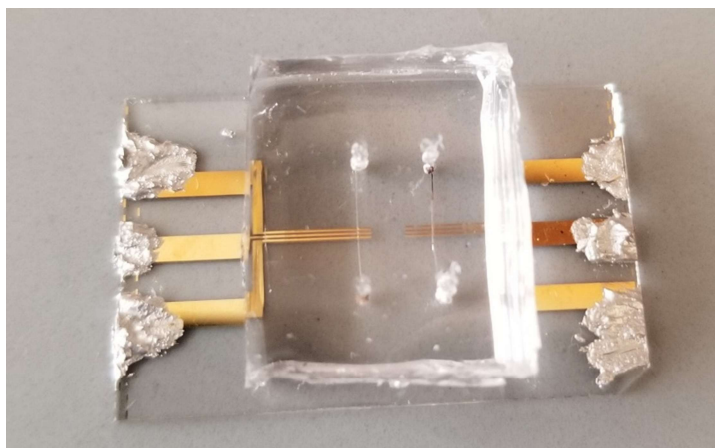
Figure 3.5: Image of Covalently Bonded Electrical and Microfluidic Subsystems

Integration of the magnetic subsystem at this point is very simple, as the inherent magnetic attraction between the two permanent magnets on either side of the microfluidic channel will hold them in place once properly aligned. The magnetic field generated by these magnets will only be strong in a very limited volume of the channel as shown in Figure 2.7, so it is critical at this point to ensure that the edges of the permanent magnets are aligned just upstream of the sensing region. Misalignment at this point will result in a less distinct change in the electrical footprint of phagocytes with internalized particles and would therefore produce a sensor with poor sensitivity. If desired, extra steps can be taken to immobilize the permanent magnets once properly aligned.

Although the biosensor can be considered a complete package at this point, several additional steps are taken to more readily facilitate data collection. The electrodes are electrically

bonded to printed circuit board (PCB) via silver conductive epoxy. To achieve this, the two parts

of the epoxy are combined in a 1:1 ratio and manually mixed until homogeneous. The epoxy is

then applied to the electrodes and the PCB to form an electrically conductive bridge at each

electrode. The epoxy is then cured for 20 minutes at 65°C. This PCB serves simply as a fanout

board to individually access the electrodes in the biosensor. The PCB then connects to a simple

stripboard that has been designed to couple the three electrodes with the measurement equipment

via BNC connectors and current limiting-resistors.

3.4 Biological Sample Preparation

De-identified biological samples for device testing were obtained from the blood

pathology lab at Robert Wood Johnson University Hospital. The procured samples were whole

blood samples drawn from patients suspected of sepsis. They were originally sent to the

pathology lab to undergo serum lactate testing, and the concentration of serum lactate in each

sample was recorded upon receipt of the samples. All biological samples were processed and

analyzed within 8 hours of hospital pickup.

3.4.1 Neutrophil Isolation

For this study, neutrophils, the most abundant phagocytes present in an infected patient,

were the desired analyte and needed to be isolated from each biological sample. A thorough

isolation protocol was developed to achieve this by removing the majority of non-desired cells

from the sample. To begin, the whole blood samples were diluted by 50% with 1x phosphate-

buffered saline (PBS), which is a buffer solution used to match the pH and osmolarity normally

found in the human body. At this point, each of the following steps is performed in triplicate for

each individual sample. 0.8 mL of these diluted whole blood samples are carefully layered on top

of 0.6 mL of Ficoll Paque density gradient as shown on the left side of Figure 3.6, and the

samples are centrifuged at a centrifugal acceleration of 400g (approximately 3,920 m/s^2) for 25

minutes. The density gradient has a density that is greater than that of platelets, lymphocytes, and monocytes, but less than that of granulocytes and erythrocytes. Because of this, the samples are segregated into three distinct volumes after centrifugation as shown on the right side of Figure 3.6. Here the platelets, lymphocytes, and monocytes appear as a yellowish liquid at the top, the density gradient appears as a clear liquid in the middle, and the granulocytes and erythrocytes appear as a viscous deep red liquid at the bottom. The cells of interest are part of the granulocyte population in the lower volume of the sample, so the top two volumes can be removed and discarded at this point.
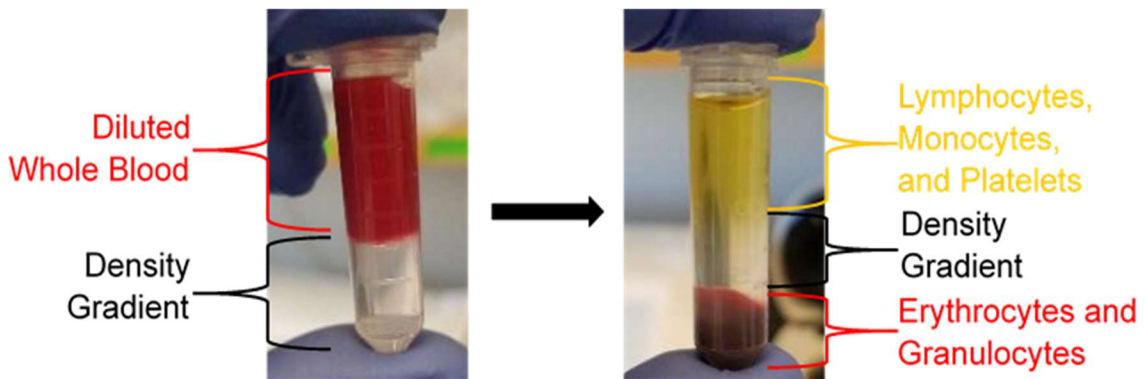
Figure 3.6: Whole Blood Samples Before (left) and After (right) Centrifugation with a Density Gradient

At this point, the remaining volume of each sample contains two distinct populations: granulocytes and erythrocytes. The neutrophils that are the desired analyte for this study are contained in the granulocyte population, so the erythrocytes must be removed. Because erythrocytes are generally more sensitive to changes in tonicity, they can be selectively lysed while leaving the majority of the granulocytes intact. To do this, 1 mL of de-ionized water is mixed into the sample, providing a hypotonic environment in which the erythrocytes are quickly lysed. After approximately 20 seconds, 0.1 mL of 10x PBS is mixed into the sample. 10x PBS is a buffer solution with a salt concentration 10 times higher than that of 1x PBS, so this restores the tonicity of the sample to its normal levels and quenches the lysing process. The sample is then centrifuged again at a centrifugal acceleration of 300g (approximately 2,840 m/s^2) for 5 minutes

to aggregate the granulocytes at bottom of the sample. This lysing process may need to be repeated several times in order to fully lyse the erythrocyte population. Once the majority of the erythrocytes have been lysed, any remaining debris is discarded, and the remaining granulocytes are suspended in RPMI 1640 cell growth medium. Although this population contains neutrophils, basophils, and eosinophils, neutrophils are present in the body in a much higher quantity than the other two cell types, so the final sample population can be assumed to contain mostly neutrophils.

3.4.2 Microparticle Internalization

At this point, one portion of the neutrophils from each sample is used for the fluorescent assay explained in the next section, another portion is introduced to the opsonized ferromagnetic microparticles to serve as the experimental population for biosensor data collection, and the rest of the neutrophils are set aside to serve as the control population for biosensor data collection. The experimental population of each sample is divided into 3 wells of a 24-well plate such that approximately 200,000 cells are present in each well suspended in 0.5 mL of RPMI. In order to achieve this, the concentration of the population must first be manually counted using a hemocytometer. AbraMag anti-human IgG coated magnetic beads are introduced to each well containing neutrophils from the experimental population in a target-to-effector ratio of 25:1. The neutrophils and opsonized ferromagnetic microparticles are allowed to incubate for 40 minutes at 37°C. Any excess ferromagnetic particles that were not phagocytosed are removed from the wells and discarded. The experimental population is removed from the wells and suspended in 0.5 mL of 1x PBS to be tested.

3.5 Fluorescent Assay

Due to the size of the ferromagnetic microparticles, it is not possible to visually observe their presence inside the cells of the experimental population using the optical microscopy tools available. Therefore, in order to provide confirmation that these particles have been internalized

by the neutrophils, a fluorescent assay was performed on a portion of the neutrophils from each sample. For this phagocytosis verification population, the cells were introduced to opsonized fluorescent microparticles instead of ferromagnetic ones. These fluorescent particles are of similar size to the ferromagnetic particles and coated in the same ligand. Therefore, if it can be shown that the cells of a particular sample have internalized these fluorescent particles, it can be reasonably assumed that that they would also have internalized the ferromagnetic particles when incubated simultaneously under the same conditions.

In order to perform this assay, the phagocytosis verification population of the sample is also divided into 3 wells of the 24-well plate such that 200,000 cells are present in each well suspended in 0.5 mL of RPMI. SPHERO anti-Human IgG coated fluorescent yellow particles are introduced to each well containing neutrophils from the phagocytosis verification population in the same target-to-effector ratio as was used for the ferromagnetic particles. Additionally, 2.5 μL of CellBrite cytoplasmic membrane dye is added to each well neutrophils from the phagocytosis verification population. If desired, a nuclear membrane stain can also be added at this point. These cells are then incubated simultaneously with the experimental population for 40 minutes at 37°C. Any excess fluorescent particles that were not phagocytosed are removed from the wells and discarded.

After incubation, the wells containing phagocytosis verification population are imaged using fluorescent microscopy. During this process, excitation wavelengths are emitted that excite the internalized fluorescent particles and the membrane dye(s). The particles and the dye(s) then each emit another wavelength that can be captured by a fluorescent microscope. The images containing each emission wavelength can be overlaid on top of each other to determine how many microparticles each cell imaged internalized as shown in Figure 3.7.
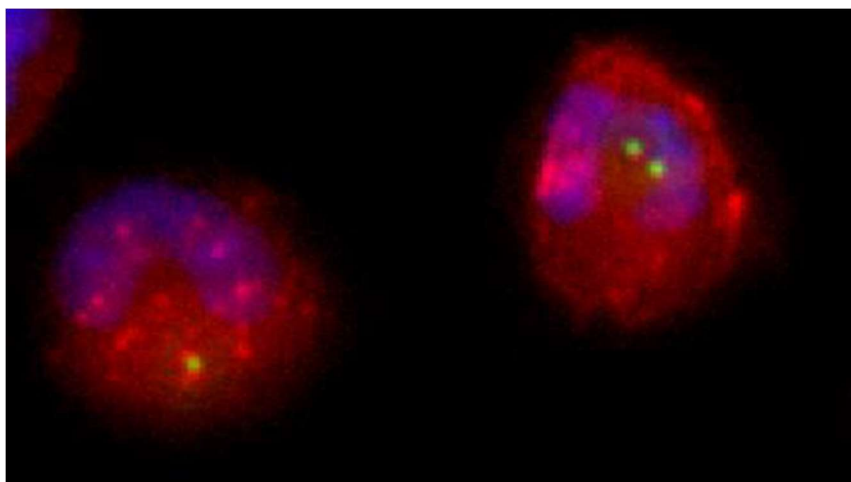
Figure 3.7: Fluorescent Image of Phagocytes (red) with Internalized Microparticles (green)

CHAPTER 4

DATA COLLECTION AND ANALYSIS

4.1 Electrical Signal Detection

The electrical signature associated with each cell that passes through the sensing region of the device is recorded by processing the information gathered by each of the two outer electrodes in the impedimetric sensor. As shown in Figure 4.1, an AC voltage signal is applied to the middle electrode, which generates an electric field between the middle electrode and each of the two outer electrodes. A current signal is then measured from each of the two outer electrodes. When each electric field is disturbed by a passing cell, an impedance is introduced between the center electrode and the corresponding outer electrode which manifests itself as a pulse in the current at that outer electrode. Since this sensor is present in a linear channel with no alternative routes, each passing cell will result in a pulse in each outer electrode current consecutively. In this way, the impedimetric sensor functions as a micro-cytometer, recording information about each cell that passes through the sensing region.
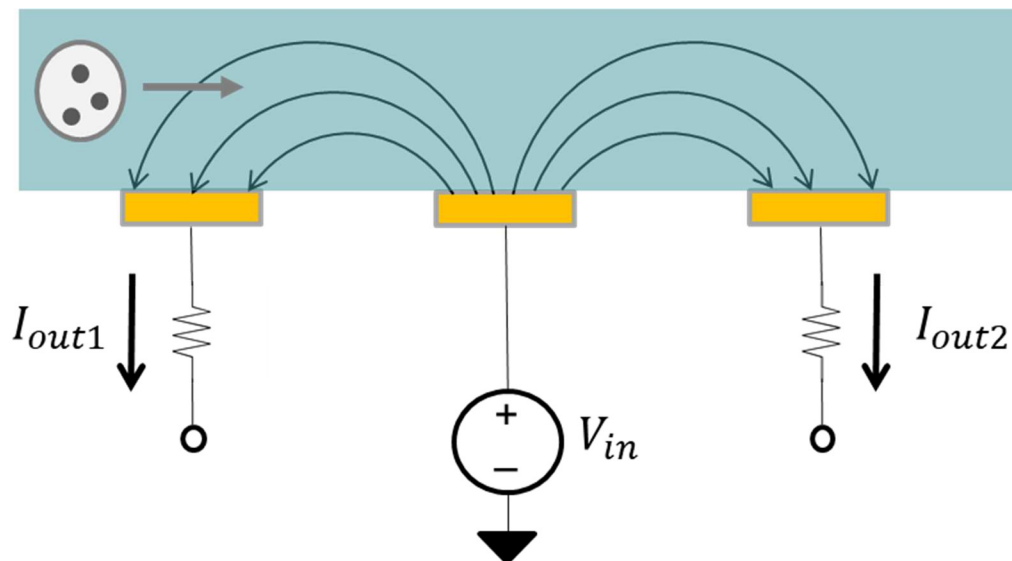

Figure 4.1: Coplanar Electrode Micro-Cytometer Diagram

4.1.1 Signal Amplification

The two current signals that carry the information relevant to each passing cell are initially too small to be analytically useful, so they must be amplified as shown in Figure 4.2. First, each current signal is passed through a transimpedance amplifier with a gain of 1,000 V/A in order to convert them to voltage signals and amplify the scales at which the signals are being analyzed. This is done using a Zurich Instruments HF2TA Current Amplifier. Then, both voltage signals are passed through a differential amplifier in order to eliminate common-mode noise and form the bipolar pulse signature described in Chapter 2. At this point, the signal is also demodulated. This is done using a Zurich Instruments HF2LI Lock-in Amplifier. At this point, the differential signal received from the lock-in amplifier is sampled at a rate of 250 kHz and recorded.
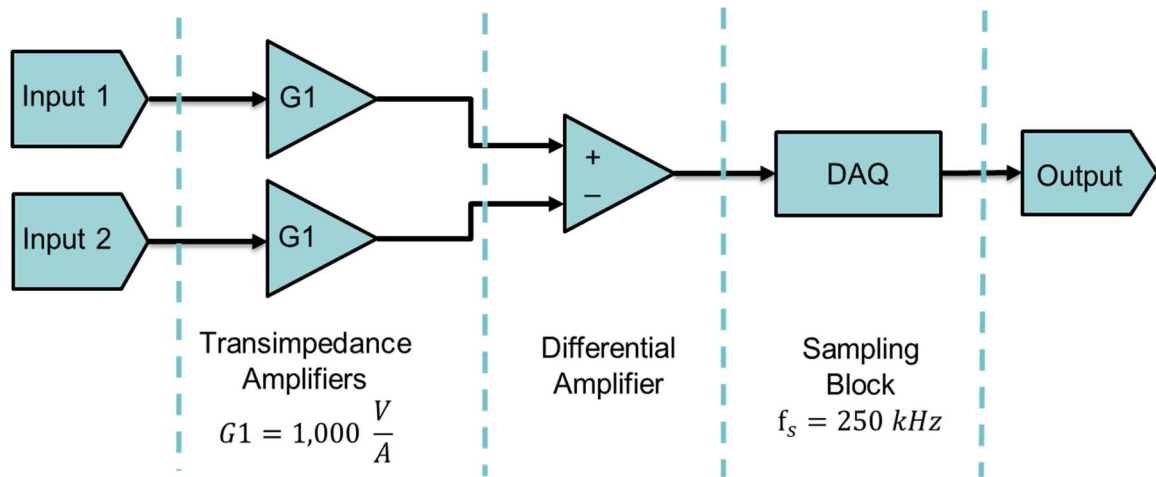

Figure 4.2: Signal Amplification Flowchart

4.1.2 Digital Signal Processing

Before analyzing the amplified and sampled voltage signal detailed in the previous section, digital signal processing techniques should be applied to the data in order to reduce the noise present in the signal and improve the ease of data analysis. Several digital filtering stages

are used to achieve this as shown in Figure 4.3. First, the sampled signal is passed through a 4th order Butterworth high-pass filter with an effective cutoff of 20 Hz. This filter eliminates any baseline drift that may be present in the signal and sets the data to a steady DC baseline of 0 V. Next, the signal is passed through a 4th order Butterworth low-pass filter with an effective cutoff of 100 kHz. This filter attenuates some of the high-frequency noise that may be disrupting the signal. Finally, the signal is passed through two 1st order Butterworth notch filters: one centered at 60 Hz and another at 120 Hz. These filters remove 60 Hz transmission line noise as well as its 120 Hz harmonic. Additional notch filters can be implemented to remove subsequent harmonic frequencies; however, they will offer diminishing returns in terms of improvements in SNR. It is important to note that 60 Hz was chosen as the appropriate transmission line frequency for testing performed in the United States, however many countries use a 50 Hz transmission line frequency, so the notch filters may have to be adjusted if testing were to be performed in another country.

Figure 4.3: Signal Processing Flowchart
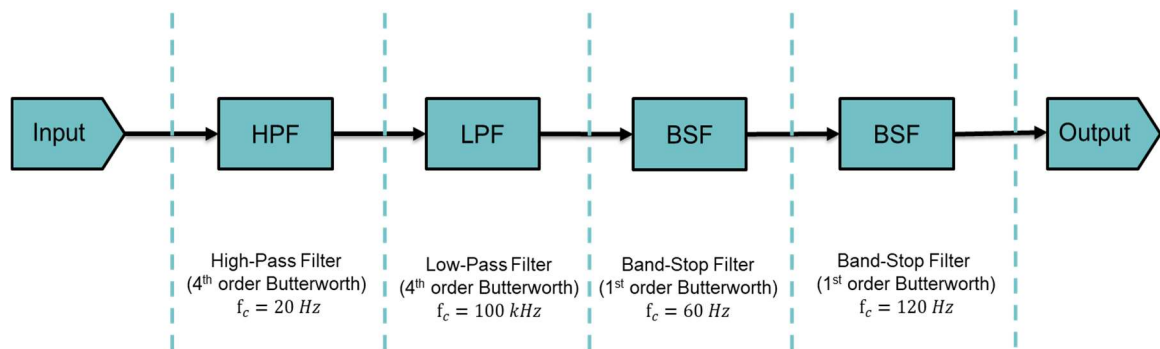
4.2 Signal Pulse Characterization and Statistical Analysis

4.2.1 Qualitative Pulse Analysis

The ultimate goal of this design was to be able to alter the flow of functional phagocytes in biological sample in such a way that it could be detected by a micro-cytometer. In order to form a preliminary surface-level qualitative determination regarding whether or not the goal was

met, several individual pulses were analyzed from both control populations and experimental

populations of the same biological samples. As can be seen in Figure 4.4, electrical pulses

generated by phagocytes that did contain internalized ferromagnetic microparticles showed

noticeably distinct electrical signatures when compared to pulses generated by phagocytes in the

control population from the same sample. While this surface-level qualitative analysis does give

some merit to the concept behind this design, it is not enough on its own to be considered a proof-

of-concept. Further data characterization is necessary.
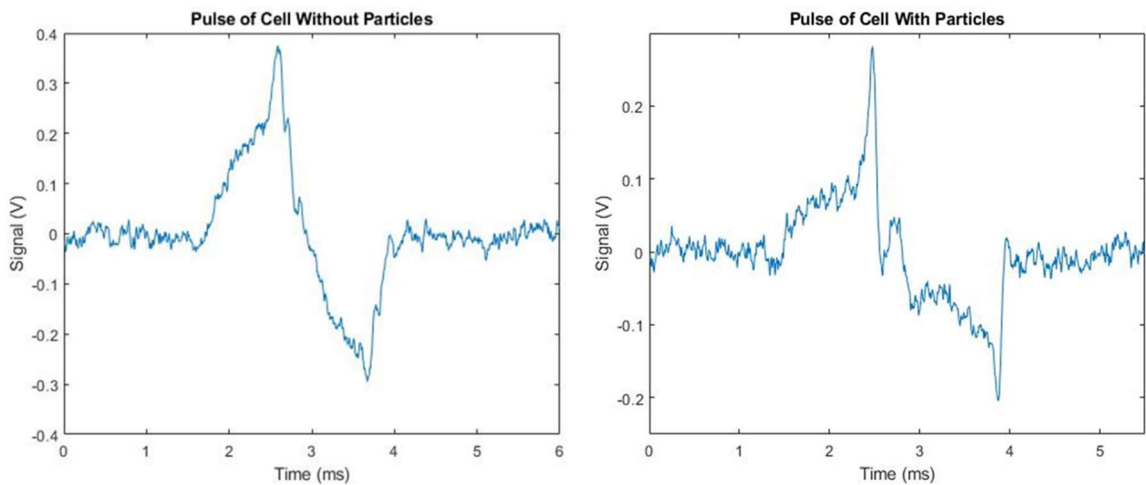
Figure 4.4: Electrical Signature Generated by a Control Population Phagocyte (left) and an Experimental Population Phagocyte (right)

4.2.2 Quantitative Statistical Analysis

In total, 17 biological samples were tested using this device. From each sample, both a

control population and an experimental population were tested, providing a total of 34 individual

datasets. In order to form a more generalized determination on the effectiveness of the proposed

biosensing framework, every pulse in each dataset collected by the device was characterized by a

uniform set of metrics and a statistical analysis was performed on those characterizations. To

determine the presence of a pulse in a dataset as opposed to electrical noise, a threshold of 50 mV

was set. An algorithm was developed to scan a complete dataset and record 5 characterization

metrics of every pulse that passed this threshold: pulse width, amplitude, rise time, fall time, and

normalized width differential factor (NWDF) as shown in Figure 4.5. The NWDF is a unique

metric defined as the normalized difference between the rise and fall times. At this time, only the

positive half of every pulse has been characterized. This was done due to technical failure that

occurred during the collection of several datasets which resulted in the loss of the negative half of

the pulse. In order to be able to keep characterization metrics uniform across all datasets,

characterizations involving the negative half of the pulse were not included. However, the

inclusion of these additional metrics may lead to improvements in the results of this biosensing

framework in the future.
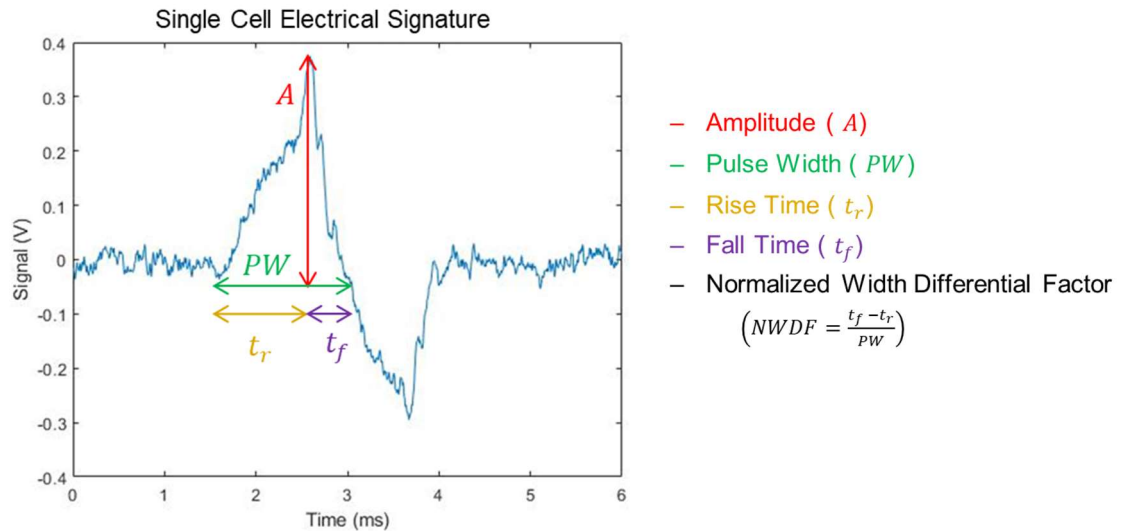
Figure 4.5: Pulse Characterization Metrics

The mean and standard deviation of all 5 characterizations were analyzed for both the

control and experimental populations in order to find a trend that could be used as a diagnostic

variable to determine whether or not a population contained phagocytes that have successfully

phagocytosed opsonized microparticles. The pulse width of every pulse is related to the speed at

which the corresponding cell is flowing. Therefore, it was originally postulated that the pulse

width alone would be able to serve as a diagnostic variable because the velocity would be

artificially altered for phagocytes with internalized ferromagnetic microparticles due to the

presence of the static magnetic field. However, this was not the case. While the mean pulse width did decrease in the experimental population as compared the control population in most of the samples tested, the standard deviation of the data was too large to confidently utilize the pulse width as a diagnostic variable. A histogram of the pulse widths in both the control and experimental populations for a single biological sample are shown in Figure 4.6.
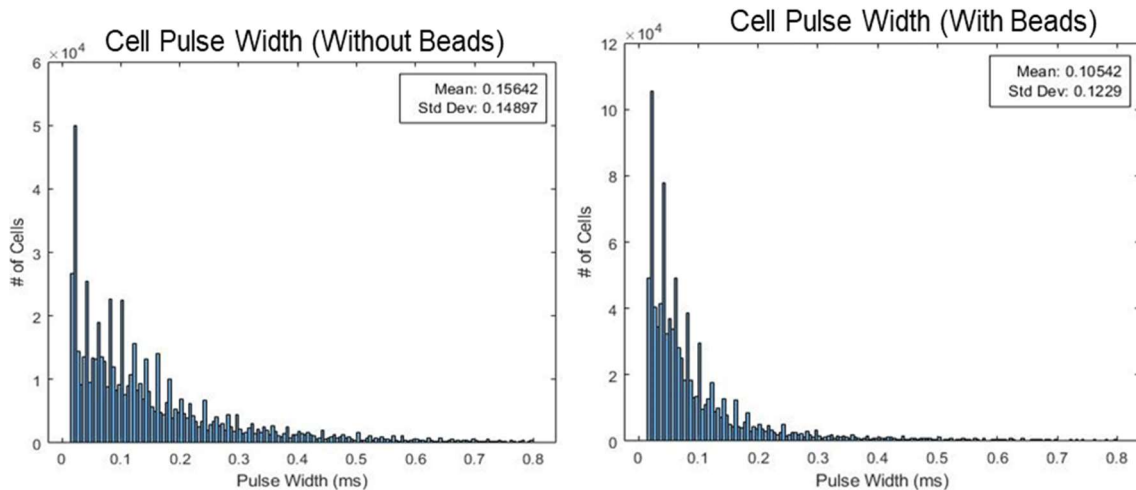

Figure 4.6: Pulse Width Histograms for Control Population (left) and Experimental Population (right) of the Same Biological Sample

Although the amplitude of the pulse was not originally postulated to serve as a diagnostic variable, it may also be altered by the presence of ferromagnetic microparticles inside a cell. The pulse amplitude is related to both the volume and the conductivity of the cell generating the pulse. Therefore, the inclusion of electrically conductive ferrous particles inside a cell may reduce the cell's amplitude by increasing its effective conductivity. For this reason, the mean and standard deviation of the pulse amplitudes for both control and experimental populations of all biological samples were also analyzed. However, the results were similar to the results derived from the pulse width analysis. Although the amplitude did indeed decrease in the experimental population as compared to the control population in the majority of the samples tested, the standard deviation of the data was again too large to confidently use this characterization as a diagnostic variable. A

histogram of the pulse amplitudes in both the control and experimental populations of a single
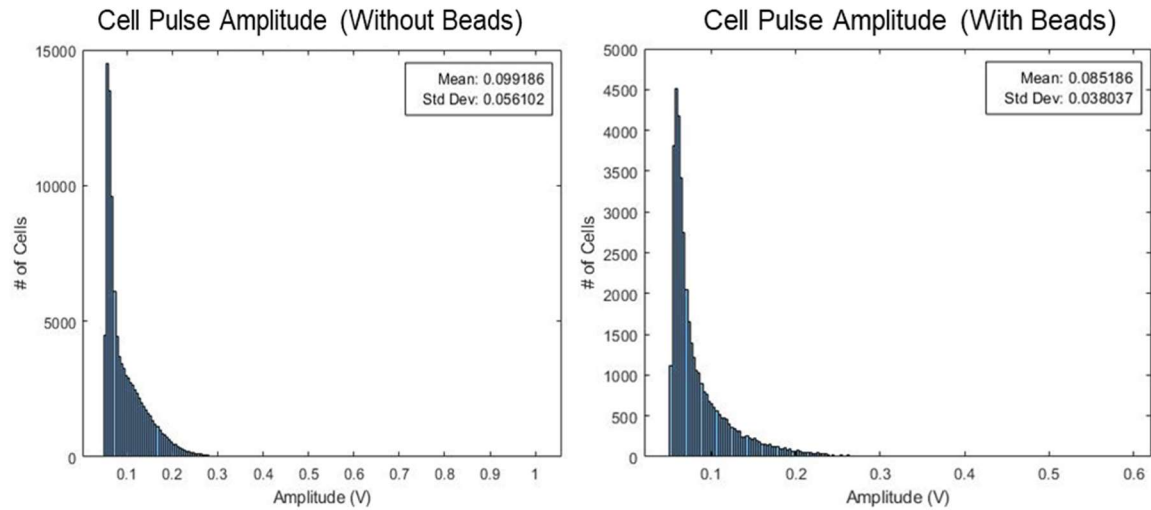
biological sample are shown in Figure 4.7.

Figure 4.7: Pulse Amplitude Histograms for Control Population (left) and Experimental Population (right) of the Same Biological Sample

Due to the fact that the quadrupole magnet configuration generates a strong magnetic

field in only a small length of the microfluidic channel, it was also postulated that the velocity of

phagocytes with internalized ferromagnetic microparticles may not be uniform throughout the

sensing region. For instance, the magnetic field may cause a phagocyte to be flowing faster at the

beginning of its pulse and slower at the end or vice versa depending on the alignment of the

magnets with the electrodes. For this reason, the pulse width of every pulse was broken down

further into three additional characterizations: the rise time, the fall time, and the NWDF as

defined earlier in this section. However, these characterizations on their own also did not prove to

be sufficient as a diagnostic variable. A paired-sample t-test was performed for all 5 characteristic

metrics and concluded that the difference between the control and experimental populations for

each metric was not statistically significant.

4.3 Neural Network Application and Results

Since no individual characterization parameter resulted in a sufficiently distinct metric for phagocytic detection and quantification, a neural network was developed to characterize the datasets based on all five metrics in conjunction in order to improve the accuracy of detection. Additionally, a second neural network was developed to serve as a sepsis diagnosis network based on data collected from the experimental populations. Both the mean and standard deviation of all 5 characterization metrics were used as inputs to the two networks, for a total of 10 input variables. The Deep Learning Toolbox on MATLAB was utilized to automatically generate, train, validate, and test both neural networks.

4.3.1 Phagocytic Detection Network

The first pattern recognition network was developed to be able to detect the presence of internalized ferromagnetic microparticles in a sample, as this would indicate that the sample contains functional phagocytes. The 10 characterization variables of all 34 datasets were used as inputs to network, and the true presence of ferromagnetic microparticles was used as a binary target for the network (1 for the experimental populations and 0 for the control populations). The binary output of the network represents the detected presence of ferromagnetic microparticles (1 if the network detects the presence of microparticles and 0 if it does not). Using the Deep Learning Toolbox, a two-layer feedforward network was created with 10 neurons and a sigmoid activation function in the hidden layer and a softmax activation function in the output layer as shown in Figure 4.8. The 34 available datasets were divided as follows: 60% for training, 20% for validation, and 20% for testing.
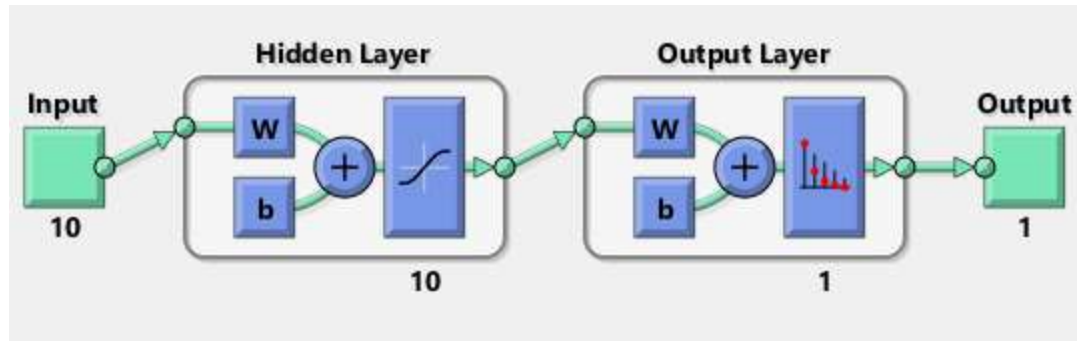
Figure 4.8: Diagram of Two-Layer Feedforward Neural Network with 10 Hidden Neurons

After training, validating, and testing this network, its performance was evaluated using two distinct tools. The first tool is called a confusion matrix, and it evaluates the number of datasets for which the target and the output were both positive (true positive), the number of datasets for which the target and the output were both negative (true negative), the number of datasets for which the target was negative and the output was positive (false positive), and the number of datasets for which the target was positive and the output was negative (false negative). Using this information, an overall success rate can be determined which defines how often the network's determination is correct according to the targets. The confusion matrix for the phagocytic detection network is shown in Figure 4.9. Of the 17 datasets that came from the control populations and did not contain any internalized ferromagnetic microparticles, 16 were correctly identified by the network. Of the 17 datasets that came from the experimental populations and did contain internalized ferromagnetic microparticles, 14 were correctly identified by the network. Thus, the success rate for functional phagocyte detection by this pattern recognition network is 88.2%.

Figure 4.9: Confusion Matrix for Phagocytic Detection Network

The second tool used to evaluate the network's performance is called a Receiver

Operating Characteristic (ROC) curve, and it is a plot used to demonstrate a diagnostic system's

performance as its diagnostic threshold is varied. With this curve, the vertical axis is taken to be

the True Positive Rate (TPR) which is defined as the proportion of actual positive cases that the

diagnostic system identifies as positive. This parameter is also known as the sensitivity of the

system. The horizontal axis is taken to be the False Positive Rate (FPR) which is defined as the

proportion of actual negative cases that the diagnostic system identifies as positive. This

parameter is related to the specificity of the system such that $FPR = 1 - specificity$. When

evaluating an ROC curve, the area under the curve (AUC) can be used as a clear metric for

pattern recognition performance in which an AUC of 1 is indicative of a perfect diagnostic

method and an AUC of 0.5 is indicative of diagnostic system which is statistically as effective as

randomly guessing an output. The ROC curve for the phagocytic detection network is shown in

Figure 4.10. This network performed with an AUC of 0.92
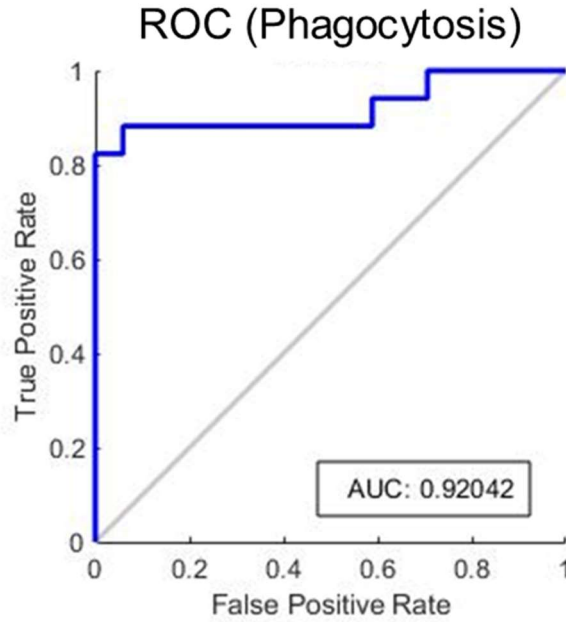
$$TPR = \frac{TP}{TP + FN}$$

(sensitivity)

$$FPR = \frac{FP}{FP + TN}$$

(1 − specificity)

Figure 4.10: ROC Curve for Phagocytic Detection Network

4.3.2 Sepsis Detection Network

The second pattern recognition network was developed to be able to diagnose sepsis based on the phagocytic performance of a biological sample. For this network, only the characterization variables from the 17 datasets derived from the experimental populations of each biological sample were used as inputs since these datasets contain information regarding the phagocytic capability of the subject. The true sepsis diagnosis based on the serum lactate concentration of the subject as explained in Chapter 1 was used as a binary target for the network (1 for samples with lactate levels greater than or equal to 2.0 mmol/L and 0 for samples with lactate levels less than 2.0 mmol/L). The binary output of the network represents the diagnosis as determined by the network (1 if the network determines the subject is septic and 0 if the network determines the subject is not septic). The same two-layer feedforward network structure as shown in Figure 4.8 was used again for this network. The 17 available datasets were divided as follows: 60% for training, 20% for validation, and 20% for testing.

After training, validating, and testing this network its performance was evaluated using
the same tools as the previous network. The confusion matrix for the sepsis detection network is
shown in Figure 4.11. Of the 9 datasets that came from subjects with lactate levels below 2.0
mmol/L, 7 were correctly diagnosed by the network. Of the 8 datasets that came from subjects
with lactate levels greater than or equal to 2.0 mmol/L, all 8 were correctly diagnosed by the
network. Thus, the success rate for sepsis detection by this pattern recognition network is 88.2%.
Additionally, the ROC curve for the sepsis detection network is shown in Figure 4.12. This
network performed with an AUC of 0.85.

Figure 4.11: Confusion Matrix for Sepsis Detection Network

$$TPR = \frac{TP}{TP + FN}$$

(sensitivity)

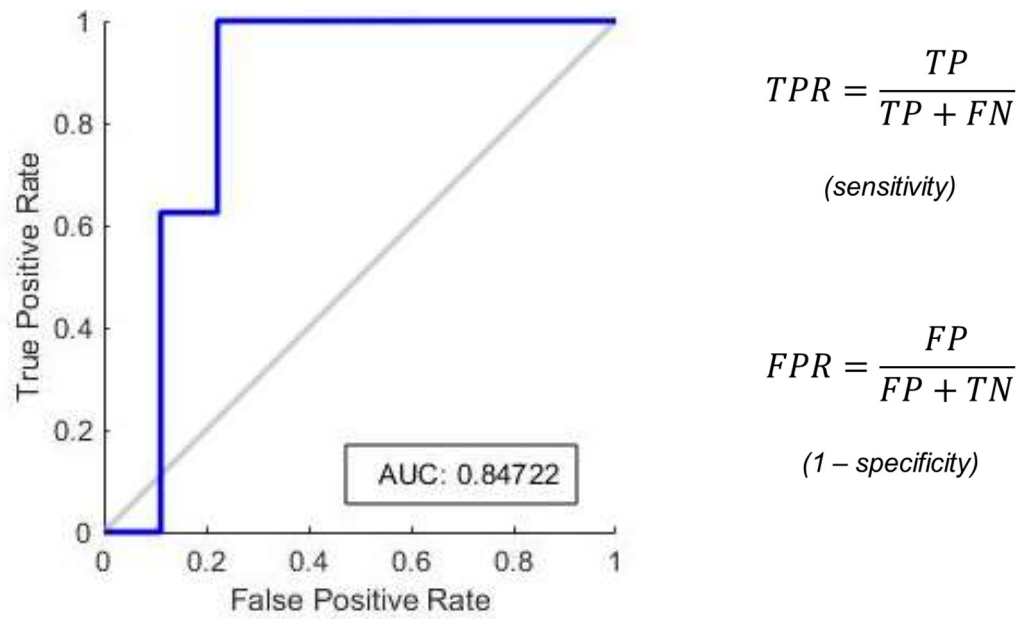$$FPR = \frac{FP}{FP + TN}$$

(1 – specificity)

Figure 4.12: ROC Curve for Sepsis Detection Network

CHAPTER 5

CONCLUSIONS AND FUTURE SCOPE

The design of a magnetic biosensing framework has been proposed in this study for use in point-of-care sepsis diagnostics and monitoring. In this design, isolated human neutrophils are introduced to opsonized ferromagnetic microparticles and passed through a novel biosensor comprised of an impedimetric micro-cytometer coupled with a microfluidic channel and a static magnetic field. Two distinct pattern recognition neural networks have been developed to analyze electrical signatures generated by neutrophils passing through the micro-cytometer. One network detects the presence of functional phagocytes in a sample and can be used for patient immunoresponse monitoring, and the other uses the phagocytic performance of the sample to detect whether or not the sample came from a septic subject and can be used for patient diagnostics. Currently, the sensing mechanism requires less than 1 mL of whole blood and approximately 2 hours to provide results (90 minutes for manual sample preparation, 25 minutes for data collection, and 5 minutes for data analysis).

Several potential future improvements to this design have been identified. First, the sensitivity of the system should be improved to be able to determine not only whether a phagocyte has internalized a microparticle, but how many microparticles it has internalized. While functional phagocyte detection is an important step towards providing clinicians with patient immunoresponse information, quantifying the phagocytic capability of the patient's immune system would be even more beneficial. Additionally, this framework should eventually be integrated into the design full POC biochip for which both biological sample processing and signal processing occur on-chip. This would hopefully result in a reduction in both the sample volume and the processing time required to receive results, increasing the clinical benefit of the framework.

In addition to design improvements, several potential future studies have also been identified. First, a clinical study should be performed using this framework to better understand its clinical relevance and performance for both diagnostic and monitoring purposes as well as other improvements that could be made to increase its benefits to clinicians. Additionally, the framework can be used in laboratory studies to identify potential therapies for the improvement of a patient's innate immunity. Monitoring the phagocytic capability of a patient's immune system under a range of both physical and biochemical stimuli could potentially lead to immunotherapies that reduce the current clinical dependence on broad-spectrum antibiotics to treat infections.

REFERENCES

[1] D. F. Gaieski, M. Edwards, K. J. Kallan, and Carr, B. G., "Benchmarking the incidence and mortality of severe sepsis in the United States," *Critical Care Medicine*, vol. 41, pp. 1167-1174, May 2013.

[2] D. Angus, et al., "Epidemiology of severe sepsis in the United States: Analysis of incidence, outcome, and associated costs of care," *Critical Care Medicine*, vol. 29, pp. 1303-1310, Jul. 2001.

[3] J. B. Barney and E. Abraham, "Sepsis: Pathogenesis," *Encyclopedia of Intensive Care Medicine¸* 2012.

[4] R. C. Bone, et al., "Definitions for Sepsis and Organ Failure and Guidelines for the Use of Innovative Therapies in Sepsis," *Chest*, vol. 101, pp. 1644-1655, Jun. 1992.

[5] S. M. Lee and W. S. An, "New clinical criteria for septic shock: serum lactate level as new emerging vital sign," *Journal of Thoracic Disease*, vol. 8(7), pp. 1388-1390, Jul. 2016.

[6] J. D. Faix, "Established and novel biomarkers of sepsis," *Biomarkers in Medicine*, Vol. 5(2), pp. 117-130, Apr. 2011.

[7] J. Baker, M. W. Nijsten, and T. C. Jansen, "Clinical use of lactate monitoring in critically ill patients," *Annals of Intensive Care*, vol. 3, 2013.

[8] R. J. Fair and Y. Tor, "Antibiotics and Bacterial Resistance in the 21st Century," *Perspectives in Medical Chemistry*, vol. 6 pp. 25-64, 2014.

[9] A. Ahmed, et al., "Biosensors for Whole-Cell Bacterial Detection," *Clinical Microbiology Reviews*, vol. 27(3), pp. 631-646, Jul. 2014.

[10] S. Campuzano, P. Yáñez-Sedeño, and J. M. Pingarrón, "Molecular Biosensors for Electrochemical Detection of Infectious Pathogens in Liquid Biopsies: Current Trends and Challenges," *Sensors (Basel)*, vol. 17(11), Nov. 2017.

[11] C. Rosales and E. Uribe-Querol, "Phagocytosis: A Fundamental Process in Immunity," *Biomed Research International*, 2017.

[12] B. Alberts, A. Johnson, J. Lewis, et al., "Molecular Biology of the Cell," 4th ed., *Garland Science*, 2002.

[13] D. M. Richards and R. G. Endres, "The Mechanism of Phagocytosis: Two Stages of Engulfment," *Biophysics Journal*, vol. 107(7), pp. 1542-1553, Oct. 2014.

[14] A. K. Lehmann, S. Sørnes, and A. Halstensen, "Phagocytosis: measurement by flow cytometry," *Journal of Immunological Methods*, vol. 243(1-2), pp. 229-242, Sep. 2000.

[15] A. H. Kampen, T. Tollersruda, S. Larsen, et al., "Repeatability of flow cytometric and classical measurement of phagocytosis and respiratory burst in bovine polymorphonuclear leukocytes," *Veterinary Immunology and Immunopathology*, vol. 97(1-2), pp. 105-114, Jan. 2004.

[16] S. K. Vashist, "Point-of-Care Diagnostics: Recent Advances and Trends," *Biosensors (Basel)*, vol. 7(4), Dec. 2017.

[17]   S. Kumar, S. Kumar, A. Ali, et al., "Microfluidic-integrated biosensors: Prospects for point-of-care diagnostics," *Biotechnology Journal*, vol. 8(11), pp. 1267-1279, Nov. 2013.

[18]   L. Gervais, N. de Rooij, and E. Delamarche, "Microfluidic Chips for Point-of-Care Immunodiagnostics," *Advanced Materials*, vol. 23(24), pp. H151-H176, Jun. 2011.

[19]   S. K. Vashist, P. B. Luppa, L. Y. Yeo, et al., "Emerging Technologies for Next-Generation Point-of-Care Testing," *Trends in Biotechnology*, vol. 33(11), pp. 692-705, Nov. 2015.

[20]   T. Astles, "Iatrogenic anaemia in the critically ill: A survey of the frequency of blood testing in a teaching hospital intensive care unit," *Journal of the Intensive Care Society*, vol. 10(4), Oct. 2009.

[21]   N. Yaacobi, M. Bar-Meir, I. Shchors, and R. Bromiker, "A Prospective Controlled Trial of the Optimal Volume for Neonatal Blood Cultures," *The Pediatric Infectious Disease Journal*, vol. 34(4), pp. 351-354, 2015.

[22]   V. Caceres, "Pinpointing value of point-of-care tests," *Ophthalmology Times*, vol. 43(4), pp. 48-49, Mar. 2018.

[23]   C. W. Seymour, T. D. Rea, J. M. Kahn, et al., "Severe Sepsis in Pre-Hospital Emergency Care Analysis of Incidence, Care, and Outcome," *American Journal of Respiratory and Critical Care Medicine*, vol. 186(12), Oct. 2012.

[24]   A. Salmanzadeh, M. B. Sano, R. C. Gallo-Villanueva, et al., "Investigating dielectric properties of different stages of syngeneic murine ovarian cancer cells," *Biomicrofluidics*, vol. 7(1), Jan. 2013.

[25]   J. Yang, Y. Huang, X. Wang, et al., "Dielectric Properties of Human Leukocyte Subpopulations Determined by Electrorotation as a Cell Separation Criterion," *Biophysics Journal*, vol. 76, pp. 3307-3314, Jun. 1999.